Dispersion of Feed Spray in a New Type of FCC Feed Injection Scheme

Zihan Yan, Yiping Fan, Zhao Wang, Sheng Chen, and Chunxi Lu
College of Chemical Engineering, State Key Laboratory of Heavy Oil Processing, China University of Petroleum, Beijing 102249, China

DOI 10.1002/aic.15047
Published online September 25, 2015 in Wiley Online Library (wileyonlinelibrary.com)

A new type of FCC feed injection scheme in which the feed is injected downward into the riser to realize a countercurrent contact of feed oil with catalyst particles is put forward. The dispersion of feed spray and flow behaviors of particles in the new type of feed injection scheme are investigated via a large scale cold-riser model. Experimental results show that the proposed scheme provides a better contact of feed oil with catalyst particles. Furthermore, the centerline equations of both the feed main flow and the secondary flow in the riser are given by introducing a density correction coefficient. The momentum-ratio of the secondary flow to the main flow is then obtained and the trajectory of the feed main jets as well as the secondary flow is estimated by the centerline equation. The computed results give a reasonable agreement with the experimental data. © 2015 American Institute of Chemical Engineers *AIChE J*, 62: 46–61, 2016
Keywords: fluid catalytic cracker riser, feed injection scheme, multiphase flow, dispersion, secondary flow

Introduction

The fluid catalytic cracker (FCC) process plays an important role in the modern refining industry. It is one of the most important processes of getting valuable products from heavy oil.[1] In an FCC reactor-regenerator system, the catalytic cracking reaction is initiated and completed in the riser reactor in a short time. The catalyst particles are contacted with vaporized feed oil in the riser and the oil is converted into light products such as gasoline, diesel, and light olefins. A riser reactor can be divided into four parts according to the different functions, that is, the prelift zone, the feed injection zone, the full reaction zone, and the quenching zone. In the feed injection system of an FCC riser reactor, the liquid feed droplets enter the riser through multiple feed atomizing nozzles. Then, they contact with the hot regenerated catalyst particles and vaporize. The resulting vapor cracks as it travels upward along with the catalysts in the riser. It is evident that the contact and flow behaviors of oil and catalyst particles in the feed injection zone of a riser will directly affect the FCC reactions.[2] In a traditional feed injection scheme, the feed oil is injected co-currently into the prelift stream to mix and react with the regenerated catalyst particles through the atomizing nozzles. The angle of the nozzles relative to the riser axis is about 30°–40° in most commercial FCC units. In an ideal condition, the atomized feed oil should contact with the catalysts rapidly and uniformly so that the maximum yield in gasoline, LPG and diesel are obtained. However, the actual flow and contact of oil with catalysts in the traditional FCC feed injection scheme are quite different from the ideal because of the very complex hydrodynamics of gas-solid flow in that zone.[3] Extensive work has been done to explore the effects of feed injection on the hydrodynamic behavior in the feed mixing zone, and it included both experimental research and numerical simulation.

Helmsing et al.[4] have found that the time of coke deposition and the primary gasoline production rates were significantly dependent on the contacting conditions and residence time of oil with catalyst particles. Al-Sherehy et al.[5] proposed a series of models for simulating the horizontal secondary gas injection into a bubbling fluidized based on their experimental results. However, those models cannot be applied to the FCC riser feed injection zone directly because of the considerable difference between a bubbling fluidized bed and a riser reactor. Marzocchella et al.[6] studied the effect of secondary air stream injected into a riser laterally. The results showed that a lateral air stream strongly affects the hydrodynamics in the regions below and above the gas inlet. E et al.[7] identified four types of jet gas concentration profiles to describe the mixing between the jets gas and prelift gas in the traditional feed injection zone. Fan et al.[8] found that a secondary flow appears near the riser wall when the feed spray is injected into the riser. The secondary flow extends at first and then it emerges into the jet main stream. The occurrence of the secondary flow is mainly because of the Kutta–Joukowski lifts exerting on feed spray by prelift gas and catalyst particles. This secondary flow promotes the mixing of oil and catalyst in the riser. However, the extension of the secondary flow also causes violent catalyst back-mixing, which is believed to be harmful to FCC reaction.

With the development of computer hardware and computational techniques, numerical simulation has become one of the most significant means of exploring the complex flow and reaction characteristics in a riser reactor and a lot of work has been carried out in recent years. Thelogs et al.[9–11] and Gao et al.[12,13] incorporated lumped kinetic models into three-dimensional (3-D) computational fluid dynamics to predict the

Correspondence concerning this article should be addressed to C. Lu at lcx725@sina.com.

performance of FCC riser reactors. The effects of the changes in the spray droplet diameter, volumetric concentration, and temperature of the feed in the feed injection zone were shown. Li et al.[14,15] simulated the gas-solid flow and catalytic cracking reactions in a FCC riser. The simulation results indicated that the feed jets velocity and the nozzle angle affected the gas-solid two-phase flow in the feed mixing zone significantly. Patel et al.[16] combined a Lagrangian description of the spray behavior with an Eulerian modeling of transport-cracking coupling in the FCC riser to understand the injection zone cracking. It was shown that precracking in the feed injection zone plays a key role in steering the overall performance of an FCC riser. Therefore, improving the contacting of oil with catalysts in the feed injection zone is very important.

A large number of studies on the gas-solid flow and reaction in the FCC feed injection zone have indicated that there are some disadvantages in the traditional feed injection system where the nozzles point upward at 30°–40° relative to the riser axis. First, concentration distribution of the catalyst particles in a riser does not match with the concentration distribution of the oil feed and this leads to a non-uniform contact between the catalyst particles and the feed oil. In addition, the residence time of oil and catalyst is quite long in some area of the feed injection zone, which leads to serious coke deposition. To overcome the disadvantages, improvements have been proposed on both the reaction process and the equipment. New reaction processes that focus on converting the low-value heavy oil into more valuable light olefins have been applied to commercial production, such as the atmospheric residue maxing gas and gasoline process,[17] the deep catalytic cracking process,[18,19] the maximizing iso-paraffins process,[20] and the two-stage-riser catalytic pyrolysis for maximizing propylene yield (TMP).[21,22] Patents covering different types of internals have been put forward for improving catalyst-feed oil contacting.[23–25] However, introducing internals in a riser can bring about other problems; for example, they can provide places for coke deposition. In Lomas and Haun's patent,[26] a hydrocarbon feed is dispersed by directing the feed jets into a flowing stream of catalyst particles in a direction substantially perpendicular to the axis of the riser to shorten the length of the contact zone of oil with catalyst particles. Li et al.[27] investigated the impact of a horizontal gas–solid jet in a high-density riser flow by CFD simulation. High speed, radially directed feed jets in the FCC feed injection system may erode the riser wall considerably if the nozzles are not absolutely symmetrically mounted. Fan et al.[28] proposed an FCC feed nozzle which can both control and utilize the secondary flow in the feed injection zone based on theoretical analysis. Mauleon and Sigaud[29] patented a process for the catalytic cracking of hydrocarbons in a fluidized bed wherein the feed is injected countercurrently to the flow of catalyst particles. Chen et al.[30] analyzed the generation and extension of the secondary flow when the feed jets come into contact with the catalyst countercurrently using the Kutta–Joukowski lift theorem. The results showed that the direction of secondary flow changes toward the riser center and it quickly mixes with the main flow when the direction of feed injection is downward. In this way, the disadvantages of secondary flow can be minimized. There is a need for more understanding of the diffusion pattern of the feed spray and the flow features of catalyst particles in the feed injection zone for the feed countercurrently injected into the catalysts flow.

In this article, the flow characteristics of gas–solid two-phase flow in the FCC feed injection zone with the feed jets contacting with the catalyst countercurrently were experimentally investigated. The influences of the nozzle angles and the operating conditions on the gas-solid flow were obtained. A method for estimating the trajectories of both the feed main flow and the secondary flow in the initial contact region of injection zone has been proposed.

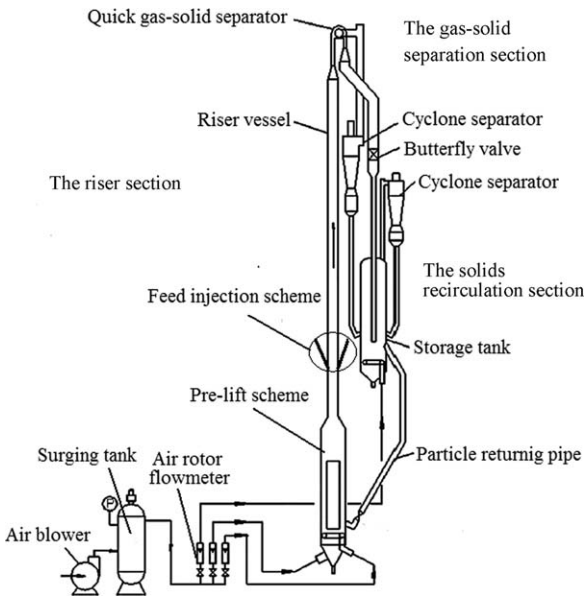

Figure 1. Experimental setup.

Experimental Setup and Measurements

Experimental setup

The experimental setup is shown in Figure 1. The system consists of a riser section, a gas–solid separation section and a solids recirculation section. The riser is 0.186 m in inner diameter and 11 m in height. Four feed nozzles are installed at a height of 4.5 m above the riser gas distributor. The nozzles are placed symmetrically in the circumferential direction, and they are pointed downward at an angle relative to the riser axis. In this way, the feed jets contact with the catalysts countercurrently in the feed injection zone of the riser. The exit cross sections of the nozzles are rectangular (40 mm × 10 mm), the same as those widely used in commercial devices.[31] Three different setting angles of nozzles ($\alpha = 150°$, 135°, and 120°) were investigated, respectively. Here, α means the angle between nozzle axis and the UPWARD direction of riser axis as shown in Figure 2. The gas–solid separation section consists of a quick gas–solid separator and a cyclone. The recirculation section includes a downer of 0.5-m ID and a butterfly valve for measuring the solid flux. The solid mass flux was calculated by measuring the time (t) for a known volume (V) of particles to accumulate on the butterfly valve after the valve was closed. Then, the solid mass flux in the riser can be obtained from Eq. 1

$$G_S = \frac{\rho_b \cdot V}{t \cdot \frac{\pi}{4} D_r^2} \tag{1}$$

Here, ρ_b is the bulk density of catalyst particles and D_r is the diameter of riser.

As the actual feed oil cannot be used in a cold model experiment directly, both the prelift gas and the injected feed were

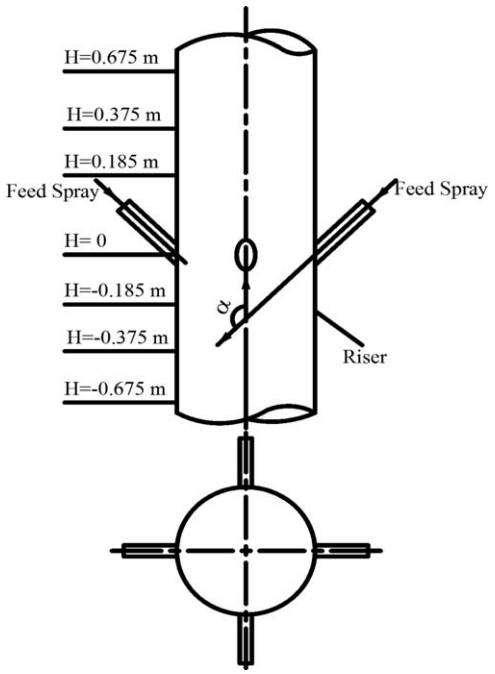

Figure 2. Scheme of the feed injection zone.

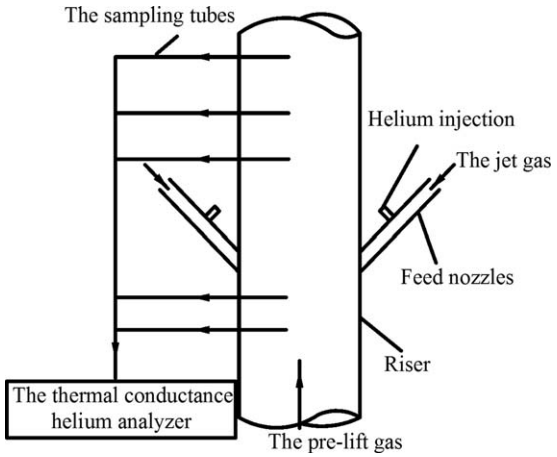

Figure 3. Sketch of the gas sampling system.

atmospheric air. The flow rates were controlled by flowmeters. In a commercial riser reactor, the feed vaporization increases the volume of gas phase considerably. However, it is quite a difficult task to simulate the vaporization of feed oil inside the industrial riser via a cold model. Therefore, we have to determine the relatively reasonable operating parameters under the limited conditions. Two facts were mainly considered in designing our experiment. The time of feed vaporization is very short in the industrial riser reactor; it is reported that the time is usually less than 0.2 s.[32] Thus, the velocities of feed jets in this experiment were close to the velocities of the vaporized feed oil in the industrial. Conversely, the total superficial gas velocity in the feed injection zone of the riser in our experiment was also in accordance with the industrial riser. In the industrial riser, the superficial gas velocity after the vaporized feed oil mixes with the prelift flow is about 7–9 m/s and the velocities of the vaporized feed oil at the exit of nozzles are usually 50–70 m/s.[12] In this article, the superficial velocity of the prelift gas ranged from 2.4 to 4.1 m/s and the gas velocities at the exit of each nozzle ranged from 41.8 to 78.5 m/s. Hence, the total superficial gas velocity in the riser ranged from 5.1 to 9.4 m/s, which can cover the operating conditions of the industry riser reactor. The solid flux in the riser was controlled in a range from 64.2 to 98.5 kg/(m^2·s). The solids used were equilibrium FCC catalyst particles whose physical properties are shown in Table 1. They are virtually the catalyst particles taken out of an industrial FCC regenerator.

Measurements and data analysis

Solids Volume Fraction and Particle Velocity. To compare the gas-solid flow behaviors in the new type of FCC feed injection scheme with those in the traditional scheme, the local solids volume fraction and the local particle velocity were measured by the same methods as the ones used by Fan et al.[8,28] A PV-6D Particle Velocity Analyzer connecting with a small probe was used to determine the local solids volume fraction and particle velocity simultaneously. The probe consists of two optical fiber sensors with a vertical distance of 2 mm. The delay time (τ) of particles passing through the tip of these two sensors was measured via the sampled signal. Then, the local velocity of particles moving in front of the probe tip was obtained by dividing the distance ($l = 2$ mm) between the two sensors by the delay time.[33,34] As to the local solids volume fraction measuring, when a beam of light irradiates a cluster of particles, part of the light will be reflected while the other part will be absorbed. The intensity of reflected light depends on the concentration of the particle cluster irradiated. The local solids volume fraction in the riser was obtained by analyzing the reflected light signal.[8]

Table 1. Properties of Tested FCC Catalyst

Particle density (kg/m^3)	1200
Bulk density (kg/m^3)	930
Mean particle size (μm)	65
Particle size range (μm)	30–90

The eigen-concentration of jet gas (corresponding to feed spray)

The feed oil terms used in this article were not real and they were replaced by atmospheric air as described above, the actually helium gas was used to simulate them. In the traditional chemical engineering, the radioactive tracer technique is usually used to explore the mechanism of chemical reactions by tracing the path that the radioisotope follows from reactants to products. However, in this article, we would determine the concentration distribution of feed injection. So the dispersion characteristic of the feed spray after it is injected into the riser from the nozzles was studied by a Helium-tracer technique[35,36] using an SR-2050 thermal conductance helium analyzer. The response time of the analyzer is $T_{90} \leq 5$ s. The local concentration of the tracer c_i at different radial locations of the riser cross section was obtained by a gas sampling system, as shown in Figure 3.

There is a significant thermal conductivity difference between the tracer gas and the sample gas. The sampled c_i might represent the characteristics of feed jets gas distribution if the injected feed jets were pure helium. However, that would require a large amount of helium for the experiment because the feed jets were injected continuously. Therefore, injecting the helium tracer into the riser via the feed jets was virtually a pulsing course rather than a continuous. In

particular, the injection time of the tracer was about 30 ms and the tracer flux was undoubtedly much less than that of the prelift gas and nozzle jets gas. The concentration c_i can only quantify the local concentration of helium in the sampled gas, rather than that in the two-phase flow. In other words, the volume of the particles is not taken into consideration if the sampled c_i is used directly. Besides, the injected amount of helium undoubtedly relates to the injecting time of helium. The concentration and the residence time of the tracer will vary with the injecting time of helium. Therefore, the eigen-concentration of jet gas C_{0i} is used to describe the characteristics of the feed jets distribution in the riser. The eigen-concentration C_{0i} is defined as

$$C_{0i}=\frac{c_i(1-\varepsilon_{pi})}{\frac{1}{A}\sum_{i=1}^{N}c_i(1-\varepsilon_{pi})A_i}\cdot\frac{Q_j}{Q_j+Q_a} \tag{2}$$

Here, $c_i(1-\varepsilon_p)$ is the actual concentration of the tracer gas in two-phase mixture and ε_{pi} is the local solids fraction obtained with the optical fiber probe. Q_j is the volumetric flow rate of jet gas from nozzles and Q_a is the volumetric flow rate of prelift gas. The term $Q_j/(Q_j+Q_a)$ is introduced to avoid the error results from the difference between the continuous feed and the pulsatile injection of the tracer. A_i is the integral area of the specific ring region and A is the total area of the cross section.

The residence time of feed jets is also an important parameter in the feed injection zone of FCC riser reactor. However, this article mainly focuses on the concentration distributions of feed jets and catalyst particles in the proposed feed injection scheme. The Helium-tracer technique was used to investigate the concentration distribution of the feed spray. Six axial measuring cross sections were determined and each cross section has six different radial measuring points. Furthermore, the residence time of helium in this experiment relates to the injecting time of helium as described above. Therefore, the residence times we obtained in this experiment are quite different from the residence time in the traditional chemical engineering. In the future work, we want to establish the connection among these residence times. It may be a connection between the Lagrange and Euler method at each measuring point.

The Catalyst-oil matching index

Similar to the jet eigen-concentration C_{0i}, the eigen-solids volume fraction ε_{0pi} is defined as

$$\varepsilon_{0pi}=\frac{\varepsilon_{pi}}{\frac{1}{A}\sum_{i=1}^{N}A_i\varepsilon_{pi}} \tag{3}$$

When the eigen-solids volume fraction and the jet gas eigen-concentration are obtained by the above methods, the contact of catalysts with oil at different locations can be characterized. A local catalyst-oil matching index λ_i and an average catalyst-oil matching index λ_m are proposed.

With the eigen-solids volume fraction ε_{0pi} and the jet eigen-concentration C_{0i}, the ratio ε_{0pi}/C_{0i} can be used to quantify the match between the catalyst particles and oil at any measured point. However, the ratio ε_{0pi}/C_{0i} probably assumes a very large value in some cases (if $C_{0i}\rightarrow 0$), thus the logarithmic function is introduced in this article to limit the values within a certain range. Then, the local catalyst-oil matching index λ_i is defined as

$$\lambda_i=\ln\left(\frac{\varepsilon_{0pi}}{C_{0i}}\right) \tag{4}$$

When the values of ε_{0pi} and C_{0i} are close to each other, the value of λ_i is closer to 0, and then the distributions of the catalysts particles and the feed jets gas are better matched. Based on λ_i, a parameter named the average catalyst-oil matching index λ_m is introduced to describe the contact of catalyst particles with oil at different axial elevations. To reflect the average value and the standard deviation of the local catalyst-oil matching index in the whole cross section at the same time, the average catalyst-oil matching index λ_m is defined as

$$\lambda_m=\frac{1}{A}\sum_{i=1}^{N}A_i\left|\frac{\varepsilon_{0pi}}{C_{0i}}-1\right|\cdot\sqrt{\frac{1}{A(N-1)}\sum_{i=1}^{N}A_i(\lambda_i-\overline{\lambda})^2} \tag{5}$$

Here, $\overline{\lambda}=\frac{1}{A}\sum_{i=1}^{N}A_i\lambda_i$, it is the average value of each λ_i in a given cross section. The term $\frac{1}{A}\sum_{i=1}^{N}A_i\left|\frac{\varepsilon_{0pi}}{C_{0i}}-1\right|$ is used to calculate the average value of local catalyst-oil matching index λ_i in the whole cross section while the term $\sqrt{\frac{1}{A(N-1)}\sum_{i=1}^{N}A_i(\lambda_i-\overline{\lambda})^2}$ reflects the fluctuations of each λ_i. Obviously, for a given cross section, a smaller value of λ_m means that the contact of oil with catalyst particles is better at that axial elevation.

Experimental Results

Flow characteristics in the new type of feed injection zone

There are six axial measured cross sections and each cross section has six radial measured points. The height at which the nozzles are installed is set as $H=0$ m and the axial location is given as positive for the measurements made above the nozzles and negative for those below the nozzles (as shown in Figure 2). The detailed axial heights H, dimensionless radial positions r/R as well as the setting angles α are shown in Table 2. It is noted that the radial measurements at any cross section were taken exactly above (or below) a nozzle in this article (the investigated radial direction is in alignment with the projection of the nozzle axis).

The radial profiles of the flow characteristics at different cross sections of the riser are shown in Figures 5–10 for a nozzle jet velocity of 78.5 m/s, a prelift gas velocity of 3.5 m/s, and a solid flux in the riser of 76.2 kg/(m^2·s). To analyze the influences of feed injection, the parameters which reflect the flow characteristics in a riser without feed nozzles are given in Figure 4. The profiles of the solids volume fraction and particle velocity present a typical core-annular structure in this case. The data were obtained in the same setup under the same operating conditions. The gas superficial velocity in Figure 4 is 6.69 m/s and the gas superficial velocity is about 6.74 m/s after the feed gas is injected into the riser in Figures 5–10.

Table 2. Values of Axial and Radial Measuring Points and Setting Angles of Nozzles

No.	1	2	3	4	5	6
H(m)	−0.675	−0.375	−0.185	0.185	0.375	0.675
r/R	0	0.25	0.5	0.7	0.8	0.95
α	150°	135°	120°			

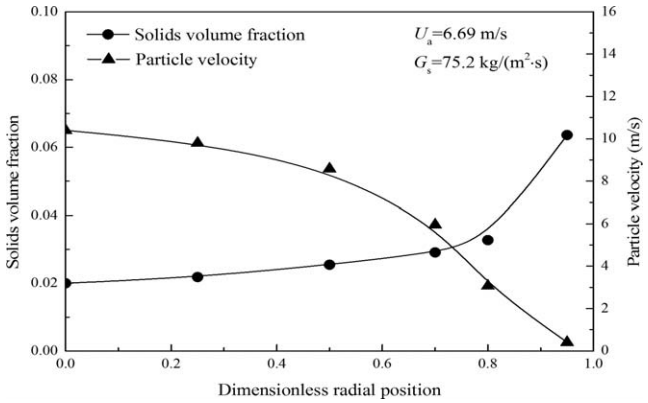

Figure 4. Measured parameters in a stable riser reactor (measurements were taken far away from the feed injection location at $H = 7.0$ m).

The cross section at H = −0.675 m

At the cross section of 0.675 m below the nozzles (No. 1 height), no helium tracer was detected for the three investigated injection angles, which indicates that the feed jets did not reach this position. Thus, only solids volume fraction and particle velocity radial profiles are presented in Figure 5. The profiles of the solids volume fraction and particle velocity distributions for the different feed injection angles are nearly similar to each other, with all showing a typical core-annular structure reported in many riser studies.[37] As for the particle velocity, it is noted that the values for $\alpha = 135°$ are decreased compared with the case of $\alpha = 120°$ near the wall of riser. This phenomenon was probably caused by the experimental error. Fortunately, the value difference is quite small as shown in Figure 5b. The trends of the particle velocity distributions for these two angles appear almost the same in the whole cross

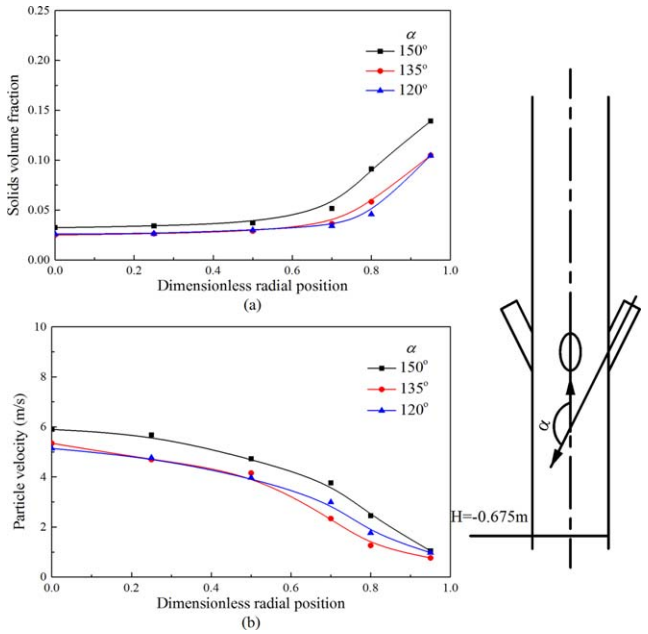

Figure 5. Measured parameters at 0.675 m below the nozzles for $U_j = 78.5$ m/s, $U_a = 3.5$ m/s, and $G_s = 76.2$ kg/(m^2·s).

[Color figure can be viewed in the online issue, which is available at wileyonlinelibrary.com.]

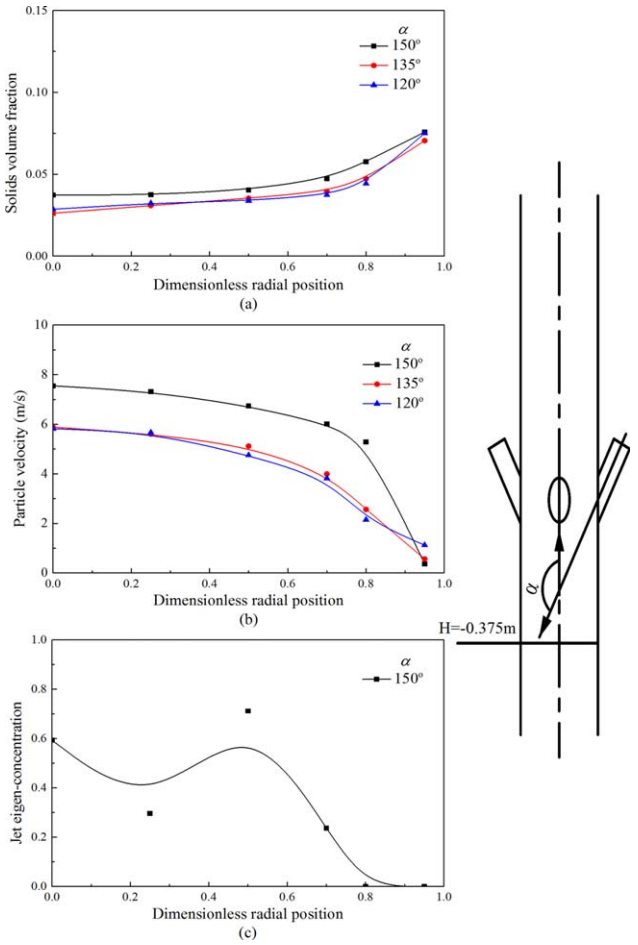

Figure 6. Measured parameters at 0.375 m below the nozzles for $U_j = 78.5$ m/s, $U_a = 3.5$ m/s, and $G_s = 76.2$ kg/(m^2·s).

[Color figure can be viewed in the online issue, which is available at wileyonlinelibrary.com.]

section, which further indicates that the jet gas has very little influence on the flow behaviors at this height.

The cross section at H = −0.375 m

At the $H = -0.375$ m cross section (No. 2 height), the tracer gas was only detected for $\alpha = 150°$ and not for the other two angles as shown in Figure 6. This is mainly because the axial component of the feed jets were large to reach this location when $\alpha = 150°$. The influence region of feed spray expands downward as the value of α increases.

The solids volume fraction profiles also show a dense layer near the wall and a dilute core area. In contrast to that at No. 1 height ($H = -0.675$ m), the solids volume fraction increases slightly in the center and decreases a little near the riser wall. The discrepancy is more significant for $\alpha = 150°$, which further indicates that the influence region of the feed spray expands farther down as the value of α increases. Because of the introduction of the feed spray, the mean particle velocity (the cross-sectional area average value) is slightly higher compared with that at $H = -0.675$ m.

The cross section at H = −0.185 m

Figure 7 shows the radial variation of the measured parameters at 0.185 m below the nozzles (No. 3 height). The helium tracer was not detected for the nozzle angle $\alpha = 120°$, which

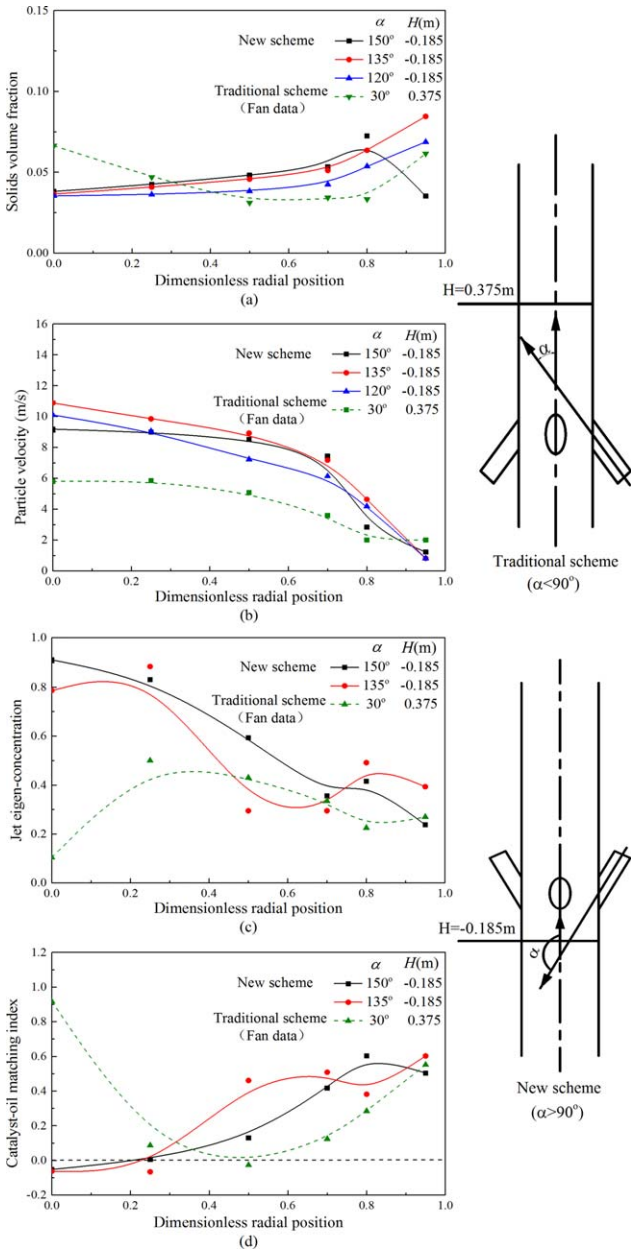

Figure 7. Measured parameters in the initial contact region of oil with catalysts for $U_j = 78.5$ m/s, $U_a = 3.5$ m/s, and $G_s = 76.2$ kg/(m^2·s).

[Color figure can be viewed in the online issue, which is available at wileyonlinelibrary.com.]

further demonstrates that the vertical length of influence of the feed spray decreases as the angle α decreases. At this cross section, the radial variations of the measured parameters were quite different from those at the other cross sections and they varied with the spray injection angle. These profiles suggest that this location is the initial contact region of oil with catalyst particles. To clearly compare the measured parameters in this region with those in the traditional feed injection scheme, the distributions of the same parameters in the initial contact region in the traditional structure (Fan et al.[8]) were also replotted in Figure 7. For traditional scheme, the measured cross section which represents the initial contact region of oil with catalysts is at $H = 0.375$ m, while in the proposed new scheme, the cross section is at $H = -0.185$ m.

Feature of the Jet. The maximum value of the jet eigen-concentration occurs at the riser center for $\alpha = 150°$ and then it decreases radially. Also a local maximal value of the jet eigen-concentration appears near the wall of the riser. The location of the peak varies with the feed injection angle. This characteristic of the jet eigen-concentration distribution demonstrates that both the main stream and the second stream of the injected feed co-exist at this cross section. The position and development of the main stream and the secondary stream are analyzed later. In this initial contact region of oil with the catalyst particles, the feed gas can be evidently detected at the whole cross section in the new type of feed injection scheme while it almost cannot be measured in the riser center in the traditional feed method. In other words, the radial dispersion of the feed spray is clearly faster than that in the traditional arrangement.

Feature of the Solid Phase. The distribution of solids volume fraction varies with the feed injection angle α at this cross section. The highest particle concentration is at the radial position of $r/R \approx 0.8$ for $\alpha = 150°$, while it is near the wall for the 135° and 120° angles. Comparing the cross section at $H = -0.185$ m with $H = -0.375$ m, the highest value of solid volume fraction is lower while the lowest local solids concentration is higher. That is to say, the catalyst particles distribute more uniformly at $H = -0.185$ m. The mean particle velocity increases a lot at the $H = -0.185$ m location under the influence of the feed spray. The uniform distribution of solids volume fraction and high-particle velocity in this area are likely favorable to the mixing and reaction of oil with catalysts.

As noted above, a secondary flow of feed spray appears near the riser wall when the feed jets are injected. As the feed spray countercurrently contacts with the prelift stream of the prelift gas and the catalysts particles, the radial component of feed jets is larger than the axial component because of the resistance exerted by the upward prelift flow. Thus, the direction of the spray main stream will be more toward the riser center. As a result, some catalyst particles will be transported to the center from the riser wall area. Conversely, the secondary flow near the riser wall will impinge on the catalyst particles and some particles may gather there. Then, a dense-phase region of particles appears. Thus, the highest value of solids volume fraction is not at the riser wall area for $\alpha = 150°$ at this cross section. The diffusion of solids in the secondary flow toward the riser center is higher when the angle α decreases. It is likely that a similar phenomenon may appear in the axial area which is closer to the nozzles for $\alpha = 135°$ and 120°. However, the specific location was not precisely determined because of the limited measured cross sections in the experiment. It should be investigated in detail in the further research.

The Match Between Particles and Jet. From Figure 7, we can see that the values of the local catalyst-oil matching index λ_i in the new type of feed injection scheme (oil contact with the catalyst countercurrently) are closer to 0 for $r/R < 0.3$, while in the traditional scheme the values are quite large at the same radial location. As a result, the average value of the catalyst-oil matching index over the whole cross section is smaller. Therefore, when the feed spray is injected downward relative to the riser axis, the contact of oil with catalysts is much better in this initial contact region, especially in the riser central area. It mostly contributes to the uniform distribution of catalyst particles as well as the rapid diffusion of the feed spray.

The cross section at H = 0.185 m

The profiles of the measured parameters at the cross section of 0.185 m above the nozzles (No. 4 height) are shown in Figure 8.

Feature of the Jet. At this cross section, there is very little variation in the jet eigen-concentration in the radial direction. The feed spray diffuses to the center of the riser and mixes with the prelift flow soon after it is injected downward into the riser. As a result, the highest value of the jet eigen-concentration appears in the center of riser at the location below the nozzles. Then, the gas–solid mixing flow moves upward in the riser. It is seen that the flowing space expands rapidly in the areas above the nozzles, which contributes to the lateral diffusion of the high-speed feed jets. This lateral diffusion of jet gas increases as the angle α decreases.

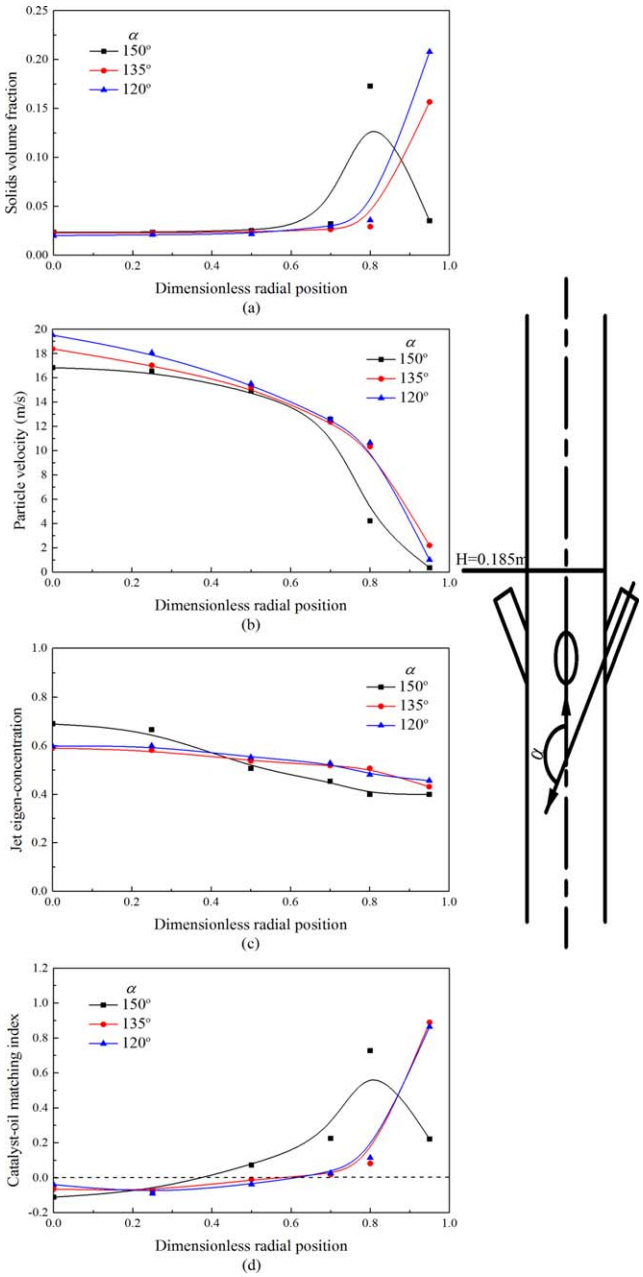

Figure 8. Measured parameters at 0.185 m above the nozzles for $U_j = 78.5$ m/s, $U_a = 3.5$ m/s, and $G_s = 76.2$ kg/(m^2·s).

[Color figure can be viewed in the online issue, which is available at wileyonlinelibrary.com.]

Feature of the Solid Phase. Similar to the case of No. 3 height ($H = -0.185$ m), the highest solids volume fraction appears at the radial position of $r/R \approx 0.8$ for $\alpha = 150°$ while it occurs near the riser wall for $\alpha = 135°$ and 120°. However, the magnitude of the solids volume fraction at this location is significantly different from those of locations below the nozzles. The solids volume fraction is much higher near the riser wall and much lower in the riser center when compared to values at locations below the nozzles. In other words, there is a greater particle concentration gradient across the riser cross section. The particle velocity decreases from the center toward the wall as was the case for locations below the spray nozzles (negative H). However, particle velocities at $H = 0.185$ m are nearly 50–100% higher than that in most of the riser cross sections. A large number of catalyst particles move toward the wall of riser under the influence of the high-speed feed jets. The high concentration of catalyst particles near the riser wall limits gas–solids mixing and cracking of oil by catalysts in industrial units. This effect is more serious when the angle α is smaller.

The Match Between Particles and Jet. The value of the local catalyst-oil matching index is quite large at radial positions $r/R \approx 0.8$–1. This is mainly because of the large number of particles gathering in the vicinity of the wall. This phenomenon is more serious when the value of α decreases (for $\alpha = 135°$ and 120°), which further indicates that the setting angle α should not be too small.

The cross section at H = 0.375 m and 0.675 m

Figures 9 and 10 show radial distributions of the measured parameters at 0.375 m (No. 5 height) and 0.675 m (No. 6 height) cross sections.

Feature of the Jet. At the $H = 0.375$ m cross section, the jet eigen-concentration close to the wall of the riser is slightly higher than in the riser core, which indicates that some lateral diffusion of feed jets gas still exists. In contrast, at $H = 0.675$ m, the jet eigen-concentration at different radial positions remains almost the same suggesting that the feed spray has fully mixed with the prelift flow at this elevation.

Feature of the Solid Phase. The radial solids volume fraction profiles for the three investigated injection angles at $H = 0.375$ m appear very similar and showing a core-annular flow structure for all the three spray angles. The values of particle velocity at this cross section are lower than those at $H = 0.185$ m. These are indications that the influence of the feed spray is no longer significant. The solids volume fraction and particle velocity profiles at 0.675 m above the nozzles are like those of a typical core-annular flow structure, which suggests that the disturbance caused by the initial interaction of feed jets gas, prelift gas, and the catalyst particles has ended. Fan et al.[8] found that the same phenomenon occurs at the height of 1.075 m above the nozzles for a traditional feed injection scheme. This shows that the influence height of feed injection above the nozzles decreases significantly when the feed jets are pointed downward into the riser.

The Match Between Particles and Jet. Comparing Figures 9 and 10 with Figure 8, it is shown that the profiles of the radial catalyst-oil matching index become more flat as the height increases. This indicates that the contact between the feed spray and catalyst particles is better as the influence of feed injection decreases. As mentioned above, the influence

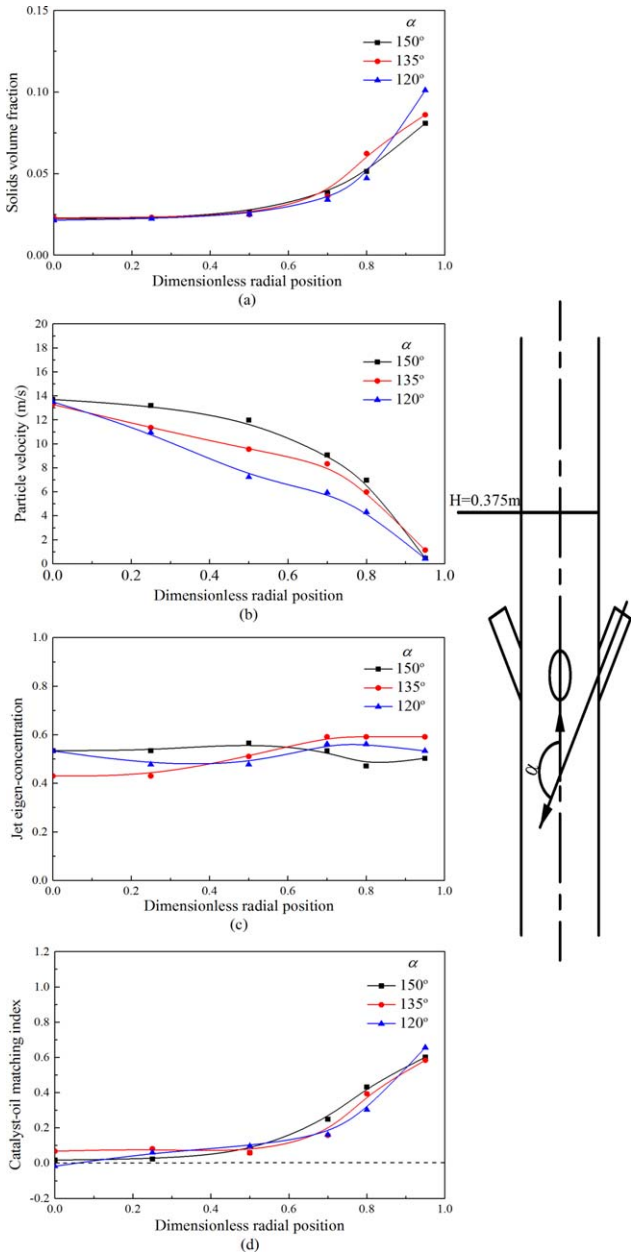

Figure 9. Measured parameters at 0.375 m above the nozzles for $U_j = 78.5$ m/s, $U_a = 3.5$ m/s, and $G_s = 76.2$ kg/(m^2·s).

[Color figure can be viewed in the online issue, which is available at wileyonlinelibrary.com.]

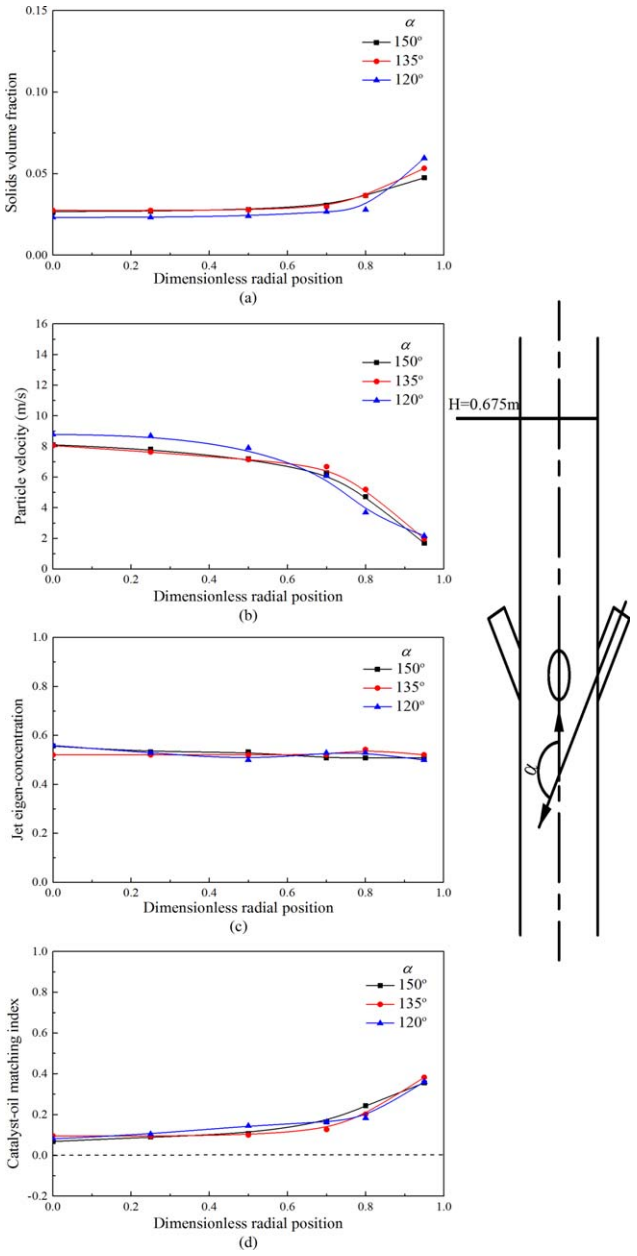

Figure 10. Measured parameters at 0.675 m above the nozzles for $U_j = 78.5$ m/s, $U_a = 3.5$ m/s, and $G_s = 76.2$ kg/(m^2·s).

[Color figure can be viewed in the online issue, which is available at wileyonlinelibrary.com.]

region of feed spray above the nozzles is shorter in the new type of feed injection scheme. Therefore, it will promote oil and catalysts interaction over a shorter riser height.

Comparison between the new scheme and the traditional

The distributions of the measured parameters at different cross sections have provided some insight into the flow characteristics for downward directed nozzles. The flow characteristics between this new type of feed injection scheme and the traditional are compared next. To take all the measured parameters into consideration, we use the average catalyst-oil matching index λ_m. As shown above, the contact between the oil and catalyst is better when the value of λ_m is small. The cross section average catalyst-oil matching index at different heights in traditional upward-pointed feed injection scheme and the new downward-pointed feed injection scheme under similar operating conditions is shown in Figure 11.

It is evident that at each height the average catalyst-oil matching index is smaller when the feed jets are injected downward into the riser. In the initial contact region of oil with catalysts (the measured cross section is at $H = 0.375$ m for the upward-pointed scheme and it is at $H = -0.185$ m for the downward-pointed scheme), the smaller average catalyst-oil matching index in the new type of feed injection scheme denotes a better contact for the feed injection and catalyst particles. It can also be seen that the average catalyst-oil matching index in the two types of feed injection schemes is nearly the same when the feed spray becomes fully mixed with the prelift

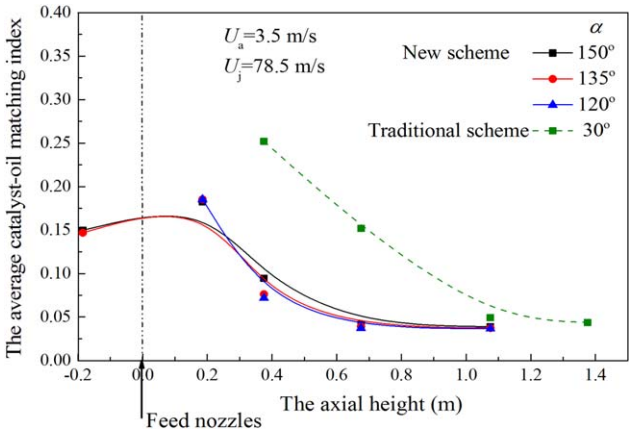

Figure 11. The average catalyst-oil matching index as function of height for downward-directed and upward-directed nozzles.

[Color figure can be viewed in the online issue, which is available at wileyonlinelibrary.com.]

gas. The average catalyst-oil matching index in the new type of feed injection scheme levels off at a height of 0.7 m while in the traditional scheme this occurs at about 1.1 m above the feed nozzles location.

It is, therefore, clear that when the feed is injected downward into the riser, the contact of oil with catalysts in the initial contact region is better than that for the upward directed feed. Also the influence height of the feed spray above the nozzles decreases considerably, which means the feed oil and catalyst particles are in a more uniform contact in the new type of feed injection scheme. However, there is another phenomenon in the new type of scheme that cannot be ignored. The average catalyst-oil matching index becomes higher in the region immediately above the nozzles before starting to decrease up the riser. At $H = 0.185$ m, the average catalyst-oil matching index is larger than at other elevations. This is likely because of high nonuniform distribution of catalyst particles in this vicinity. Therefore, the contacting of oil with catalysts will be further improved by solving this problem.

Theoretical Analysis

The centerline equation of feed spray

The hydrodynamics of gas-solid flow in the feed injection zone of a riser reactor is quite complex, which would be described by the multiple confined jets injecting into a 3-D, three-phase flow.[38] Moreover, the multiple feed jets from the nozzles and the lift gas stream meet and gather into one stream after entering the riser. This makes it quite difficult to describe the flow behaviors of the multiphase flow. If we consider a single jet injected into a large-scale riser, the situation becomes similar to that of a wall-attached jet. A similar method can also be used to quantify the centerline equation of the feed spray.[39–41] This equation can be used to reflect the trajectory of the feed jet. Then, the trajectory of the feed spray in the region where the multiple jets do not meet can be estimated. We calculate the centerline equation of the feed spray under a relatively ideal condition with the following assumptions.

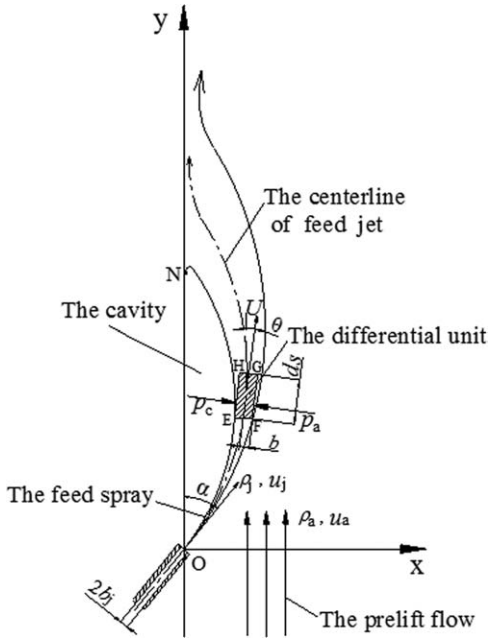

Figure 12. Modeling of the feed spray trajectories as it mixes with the prelift flow.

1. The feed spray is an incompressible 2-D flow.
2. The prelift gas–solid two-phase flow is treated as a uniform fluid.
3. The velocity of jet at the nozzle exit is uniform.

Then, a rectangular coordinate system is setup as shown in Figure 12. The origin O of the coordinate is set at the intersection of the riser wall and the nozzle axis, the positive direction of Y axis is upward and parallel to the riser axis while the positive direction of X axis is horizontal toward the riser center. The angle between the nozzle and the positive direction of Y axis is α. The average density of the prelift flow is ρ_a while the pressure and velocity are p_a and u_a, respectively. The half width of the nozzle is b_j. The velocity of jet gas at nozzle exit is u_j. The density of feed jet is ρ_j and the pressure is p_j. The average static pressure in the cavity area OEN (the area between the jet and the riser wall) is p_c. The average velocity of feed jet after it is injected into the riser is denoted by U.

Consider a condition that the jet is horizontally injected along the X axis ($\alpha = 90°$),

The equation of motion of the jet is

$$\rho u\frac{\partial u}{\partial x}+\rho v\frac{\partial u}{\partial y}=\frac{\partial \tau}{\partial y} \tag{6}$$

The boundary conditions are:

When $y = 0$, then $v = 0$, $\tau = 0$.

When $y = y_e$ (the boundary of the jet), then $u = u_a$, $\tau = 0$.

Integrating Eq. 6 on y, the integration form of the motion equation is obtained

$$\rho\int_0^y u\frac{\partial u}{\partial x}dy+\rho\int_0^y v\frac{\partial u}{\partial y}dy=\int_0^y\frac{\partial \tau}{\partial y}dy \tag{7}$$

According to Leibniz rule, Eq. 7 can be rewritten as

$$\frac{1}{2}\frac{\partial}{\partial x}\int_0^y \rho u^2dy+\int_0^y \rho v\frac{\partial u}{\partial y}dy=\int_0^y\frac{\partial \tau}{\partial y}dy \tag{8}$$

Then based on the boundary conditions, the following equation is obtained

$$\frac{\partial}{\partial x}\int_0^y \rho u^2 dy+\rho uv=\tau \tag{9}$$

The continuity equation of jet is

$$\frac{\partial(\rho u)}{\partial x}+\frac{\partial(\rho v)}{\partial y}=0 \tag{10}$$

Integrating Eq. 10

$$\rho v=-\frac{\partial}{\partial x}\int_0^y \rho u dy \tag{11}$$

Substituting Eq. 11 into Eq. 9

$$\frac{\partial}{\partial x}\int_0^y \rho u^2 dy-u\frac{\partial}{\partial x}\int_0^y \rho u dy=\tau \tag{12}$$

According to the boundary conditions, Eq. 12 is then expressed as

$$\frac{\partial}{\partial x}\int_0^{y_e} \rho u(u-u_a) dy=0 \tag{13}$$

Integrating Eq. 13

$$\int_0^{y_e} \rho u(u-u_a) dy=C \tag{14}$$

It can be concluded from Eq. 14 that the relative momentum between the jet and the surrounding fluid is a constant at the cross section along the centerline of jet. More generally, in this system the total momentum of the jet between any two cross sections does not vary with time. So the following equation is obtained

$$\frac{d}{dt}\int_V \rho u dV=0 \tag{15}$$

Here, V is the volume of jet between two cross sections.

The dynamic differential equation for any given differential element with the variable mass can be described by

$$m\frac{dv}{dt}-F^{(e)}=u_r\frac{dm}{dt} \tag{16}$$

Here, $F^{(e)}$ is the principal vector of the external force and u_r is the relative velocity.

Then for this element the following equation is obtained

$$\frac{d}{dt}\int_V \rho u dV=\sum F^{(e)}-\int_A \rho u(u_r dA)=0 \tag{17}$$

The jet momentum entering and leaving a selected differential unit (Denoted by EFGH in Figure 12) per unit time is described by

$$\int_A \rho u(u_r dA)=QU-Q_j u_j=2b\rho_j U^2-2b_j\rho_j u_j^2 \tag{18}$$

When the effect of gravity is neglected, combining Eqs. 17 and 18, the following equations are obtained

$$-(p_a-p_c)y=2b\rho_j U^2\sin\theta-2b_j\rho_j u_j^2\sin\alpha \tag{19}$$

$$[(p_a-p_c)+\frac{1}{2}C_n\rho_a u_a^2]x=2b\rho_j U^2\cos\theta-2b_j\rho_j u_j^2\cos\alpha \tag{20}$$

The term $\frac{1}{2}C_n\rho_a u_a^2$ is the kinetic pressure, the dynamic pressure of the main flow on the differential unit.

Divide Eq. 19 by Eq. 20

$$\tan\theta=\frac{dx}{dy}=\frac{2b_j\rho_j u_j^2\sin\alpha-(p_a-p_c)y}{2b_j\rho_j u_j^2\cos\alpha+(p_a-p_c+0.5C_n\rho_a u_a^2)x} \tag{21}$$

When a jet with a unit width is horizontally injected along the X axis, its volume flow rate at any cross section is calculated by

$$Q=\int_{-\infty}^{+\infty} u dy=2\int_0^{+\infty} u dy \tag{22}$$

According to Eq. 11, the entrainment velocity of the jet v_e is

$$v_e=\frac{d}{dx}\int_0^{+\infty} u dy \tag{23}$$

Combining (22) and Eq. 23, the entrainment velocity of the jet can also be written by

$$v_e=\frac{1}{2}\frac{dQ}{dx} \tag{24}$$

Then taking the width of jet into consideration, the velocity change of the jet caused by the entrainment is

$$dv=\frac{1}{2}\frac{dQ_a}{dA} \tag{25}$$

So the pressure difference between the main flow and the cavity is

$$\Delta p=p_a-p_c=\rho_a(\Delta v)^2=\rho_a\left(\frac{1}{2}\frac{\Delta Q_a}{\Delta A}\right)^2=0.25\rho_a u_a^2 \tag{26}$$

The centerline equation of the feed spray in an ideal condition is then obtained as

$$x=\frac{-C\pm(C^2+2ADy-BDy^2)^{0.5}}{D} \tag{27}$$

Here,

$$A=2b_j\rho_j u_j^2\sin\alpha$$
$$B=0.25\rho_a u_a^2$$
$$C=2b_j\rho_j u_j^2\cos\alpha$$
$$D=0.25\rho_a u_a^2+0.5C_n\rho_a u_a^2\ (C_n\approx 1\text{–}3)$$

The prelift flow in the riser is not uniform in the actual condition. The prelift gas–solid two-phase flow has a core-annular pattern with a high density near the riser wall and a low density in the riser core. As the feed spray is injected from the riser wall, the density of the main flow is higher than the average value ρ_a. Therefore, the theoretical value x calculated from Eq. 27 cannot be directly applied to the FCC feed injection system and it needs to be modified. Moreover, the parameters which reflect the gas-solid flow features of the prelift gas inevitably vary with locations. As a result, the pressure difference between the main flow and the cavity OEN also changes. This makes it quite difficult to modify Eq. 27 by a pure theoretical arithmetic. To estimate the trajectory of feed spray in the initial contact region of feed injection zone, a density correction coefficient K_D is introduced to modify Eq. 27. Then, the following equation is obtained

$$\hat{x}=\frac{1}{K_D}\cdot\frac{-C\pm(C^2+2ADy-BDy^2)^{0.5}}{D}=\frac{1}{K_D}x \tag{28}$$

The theoretical value x is calculated by Eq. 27 and the modified value $\hat{x}$ can be obtained by experiments. In the region

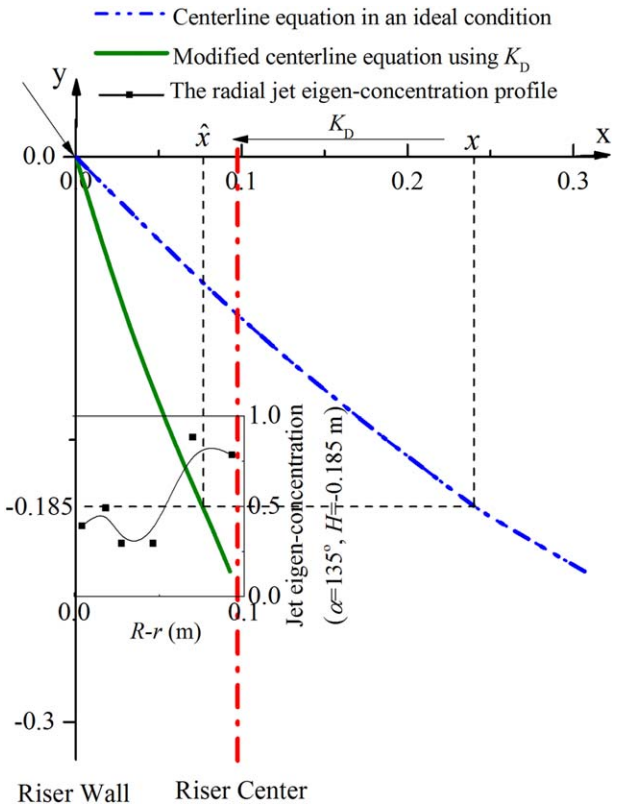

Figure 13. Example of the relationship among the theoretical centerline equation, the modified centerline equation, and the radial jet eigen-concentration profile.

[Color figure can be viewed in the online issue, which is available at wileyonlinelibrary.com.]

where the multiple feed jets have not met with each other, the location of the centerline of the feed spray in a cross section represents a radial maximum value of the jet eigen-concentration. The modified value $\hat{x}$ is obtained according to

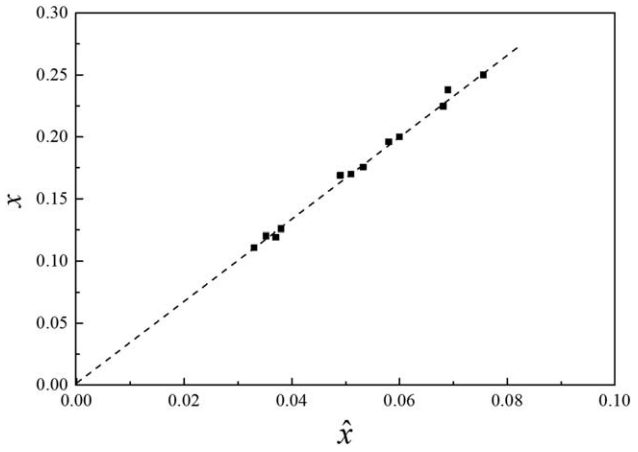

Figure 14. The density correction coefficient K_D obtained from experimental data.

the profile of the radial jet eigen-concentration. Then, the density correction coefficient K_D is acquired based on the theoretical value x and the modified value $\hat{x}$.

Figure 13 gives an example of the relationship among the theoretical centerline equation, the modified centerline equation and the radial jet eigen-concentration profile. According to Eq. 27, in an ideal condition the theoretical value x can be calculated when the axial height y is known. The modified value $\hat{x}$ is obtained from the radial jet eigen-concentration profile as noted above. Then, we can gain the density correction coefficient K_D by Eq. 28. A series of values of K_D were gotten when the operating conditions and the setting angles of nozzles varied, as shown in Figure 14. From Figure 14, we can see that the values of K_D are nearly a constant under different conditions, indicating that a linear relationship of x to $\hat{x}$ exists in this system. The modified centerline equation (Eq. 28) is found according to the density correction coefficient K_D, and then, the value of $\hat{x}$ at any axial cross section can be calculated. The calculated data are compared with the experimental result, as shown in Figure 15.

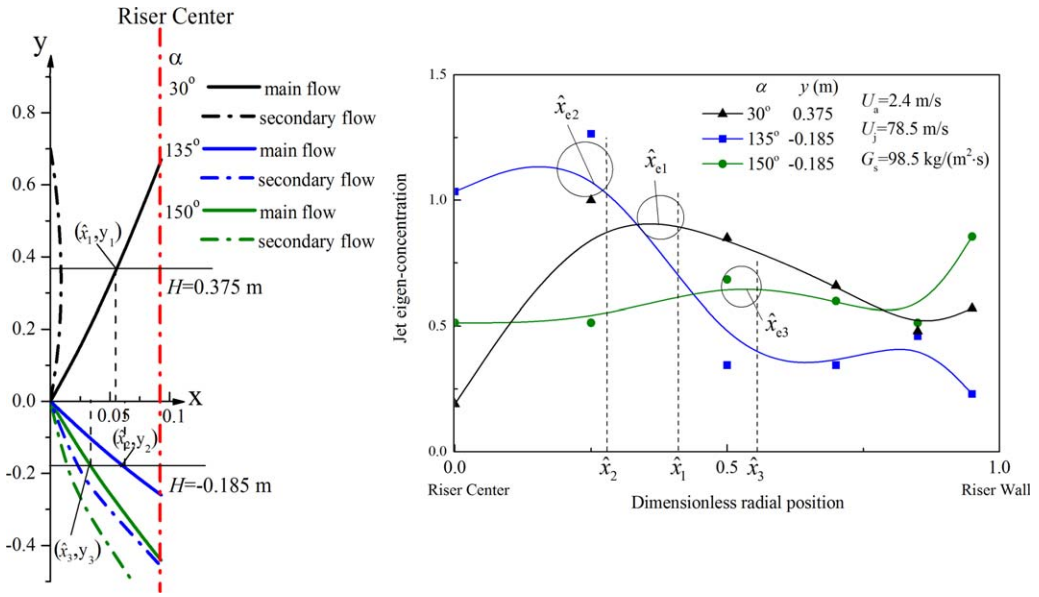

Figure 15. Comparison of the calculated $\hat{x}$ values with the radial jet eigen-concentration profiles.

[Color figure can be viewed in the online issue, which is available at wileyonlinelibrary.com.]

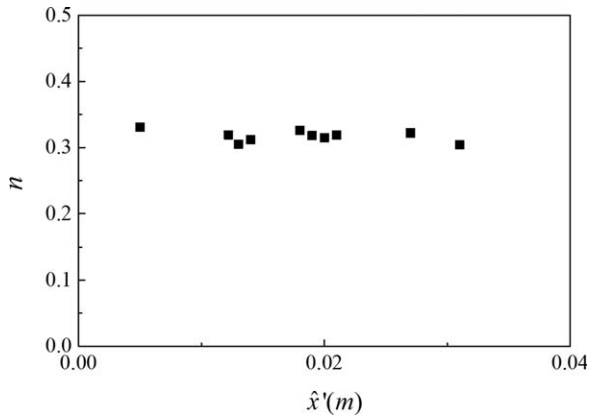

Figure 16. The ratio *n* obtained from experimental data.

It is necessary to point out that this analysis is only applicable to the region where the multiple feed jets have not met with each other. Fortunately, the gas-solid flow behaviors in this relative small region have some common characteristics even if the feed injection angle changes.

In Figure 15, $\hat{x}_i$ represents the calculated value and $\hat{x}_{ei}$ represents the experimental data. It can be seen that the calculated value and the experimental data are in a fairly good agreement. Furthermore, the modified center equation of feed spray (Eq. 28) could be used to estimate the trajectory of feed spray in the region of the feed injection zone where the multiple feed jets have not met with each other.

Fan et al.[8] pointed out that a secondary flow occurs near the riser wall when the feed spray is injected into the riser. The velocity of secondary flow is smaller than that of main flow. The orientation of the secondary flow relative to that of the main stream was found to satisfy the following equation[28]

$$\tan\alpha=\frac{1}{3}\tan\beta \tag{29}$$

Therefore, as done above, the centerline of the secondary flow can also be obtained if its velocity at the nozzle exit is known. However, the relationship between main stream and secondary flow velocities cannot be exactly obtained because of the complex gas-solid flow characteristics in the feed injection zone. In Eq. 27, only terms A and C are related to the properties of jet flow. Notice that, the momentum of the main stream $M_I=2b_j\rho_j u_j^2$ is considered the terms A and C. Assuming that the momentum of main stream and secondary flows satisfies the following equation

$$M_{II}=nM_I \tag{30}$$

Here n is the momentum ratio of the secondary flow to the main flow.

Then, the centerline equation of secondary flow can be described by

$$\hat{x}'=\frac{1}{K_D}\frac{-C_{II}\pm(C_{II}^2+2A_{II}Dy'-BDy'^2)^{0.5}}{D} \tag{31}$$

Here,

$$A_{II}=2nb_j\rho_j u_j^2\sin\beta$$
$$C_{II}=2nb_j\rho_j u_j^2\cos\beta$$

As mentioned in the experimental results section, a local maximum value of the jet eigen-concentration appears near the wall of the riser after the feed spray is injected. This characteristic of the jet eigen-concentration distribution demonstrates that the secondary flow forms accompanying the main stream of the feed spray. Therefore, based on the radial profile of the jet eigen-concentration, the location of secondary flow at the cross section can be found. The ratio n is then obtained from the experimental value of $\hat{x}'$ and $\hat{x}$. Figure 16 gives the calculated results of n.

It is clear from Figure 16 that there is not much difference in the value of n for different injection angles and operating conditions. Thus, the terms A_{II} and C_{II} can be calculated using the average value of n. Finally, the trajectory of secondary flow is obtained using Eq. 31. The calculated value of $\hat{x}'$ is compared with the experimental data, as shown in Figure 17. It can be seen that the calculated value is in a reasonable agreement with the experimental result.

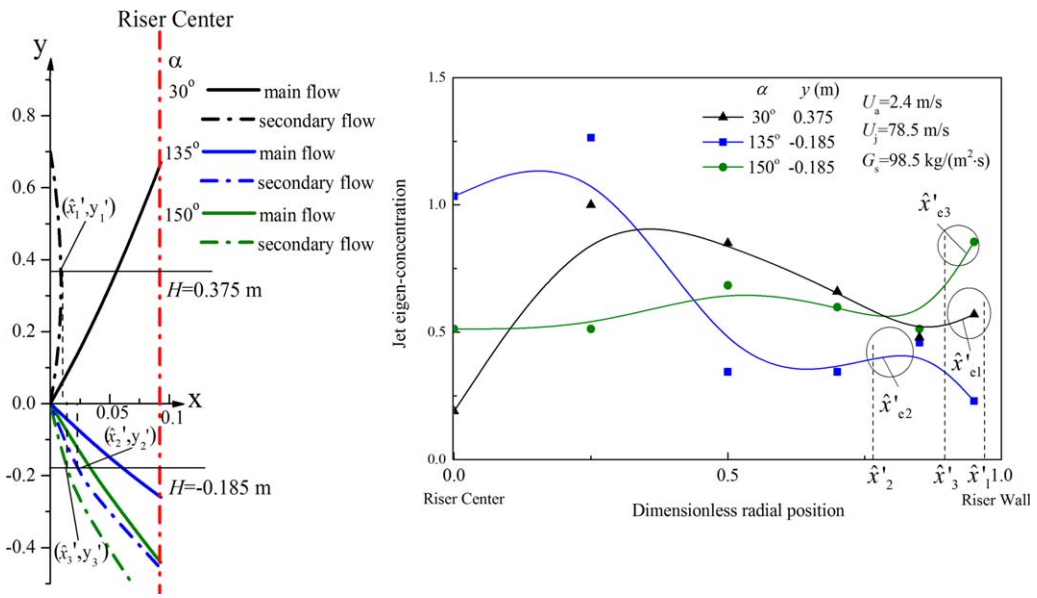

Figure 17. Comparison of the calculated $\hat{x}'$ values with the radial jet eigen-concentration profiles.

[Color figure can be viewed in the online issue, which is available at wileyonlinelibrary.com.]

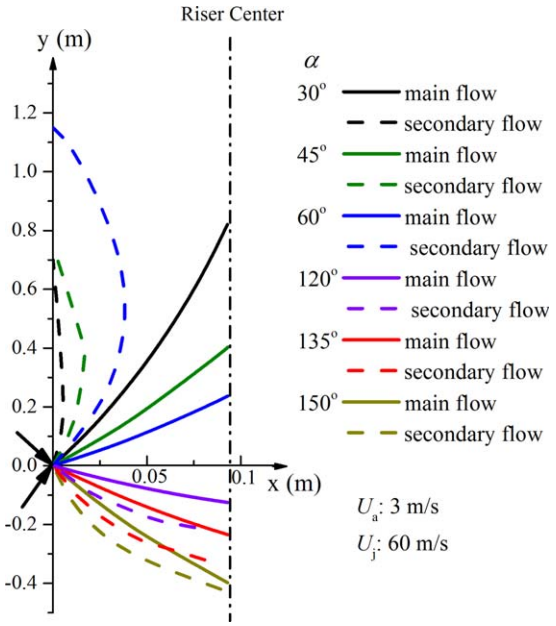

Figure 18. Predict trajectories of the main and secondary flows for different nozzle angles.

[Color figure can be viewed in the online issue, which is available at wileyonlinelibrary.com.]

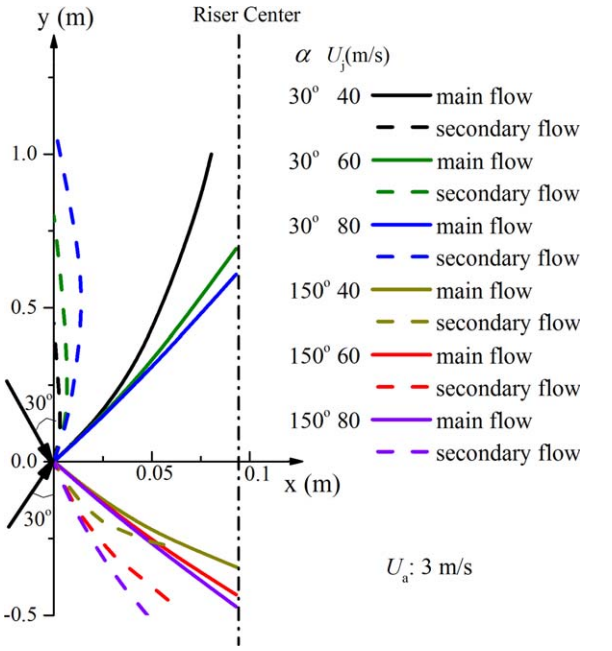

Figure 19. The calculated spray trajectories for different nozzle jet velocities at a prelift gas velocity of 3 m/s.

[Color figure can be viewed in the online issue, which is available at wileyonlinelibrary.com.]

The estimated results under different conditions

Based on the analysis above, if the radial profile of the jet concentration in the region where multiple feed jets do not meet with each other is given, the density correction coefficient K_D and the momentum ratio n between secondary flow and main stream can be calculated. Then, the trajectory of the feed spray in the initial region of feed injection zone under other conditions (different injection angles or velocities of prelift gas and feed spray) can be estimated using the obtained K_D and n. Figures 18–20 give the predicted trajectories for different conditions using the K_D and n given above.

It can be seen from Figure 18 that the trajectory of the feed flow is toward the center of the riser irrespective of whether the nozzles are installed upward or downward.

The trajectory of secondary flow, however, depends on whether the feed spray is injected upward or downward. When the nozzles are installed upward ($\alpha < 90°$), the secondary flow moves toward the riser wall and a cavity forms. Simultaneously catalyst particles are carried to this region by the secondary flow. Then, a wall dense-phase region of particles occurs there. Intense particle back-mixing was found to occur in this region.[8] The influence region of the secondary flow becomes larger when the angle between the nozzles and the riser axis increases.

When the nozzles are installed downward ($\alpha > 90°$), the direction of the main and secondary flows are toward the riser center as shown in Figure 18. As the directions of main stream and secondary flow are both toward the riser center, catalyst particles are transported to the riser core region, which makes the contact between oil and catalysts better. The secondary flow promotes the mixing of oil with catalyst particles in the initial region of feed injection zone. Fan et al.[28] and Chen et al.[30] reported similar findings. It is likely that when the injection angle α is too small, the secondary flow will immediately mix with the main flow which removes the role of the secondary flow in promoting the contact between the feed oil and the catalyst particles. Angle α of 135°–150° is proposed here when the nozzles are installed downward to fully utilize the secondary flow.

Figures 19 and 20 show the influence of operating conditions on the feed spray trajectory. In Figure 19, the prelift gas velocity is set 3 m/s and the nozzle spray velocity is varied

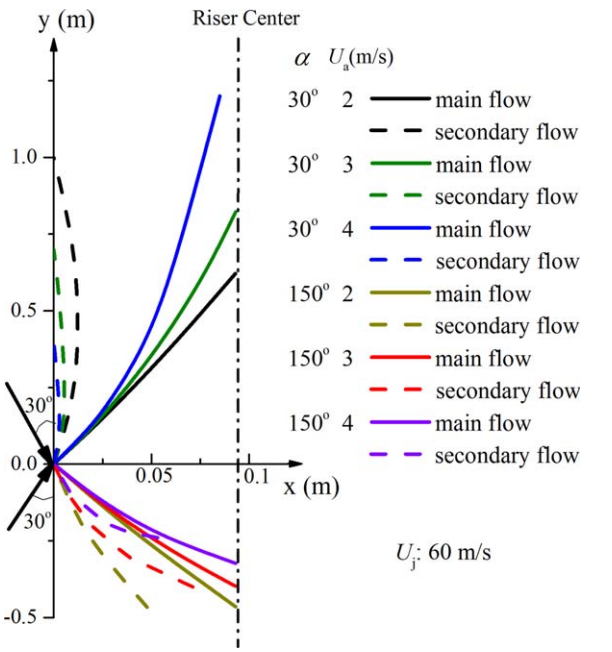

Figure 20. The calculated spray trajectories for different prelift gas velocities at a spray gas velocity of 60 m/s.

[Color figure can be viewed in the online issue, which is available at wileyonlinelibrary.com.]

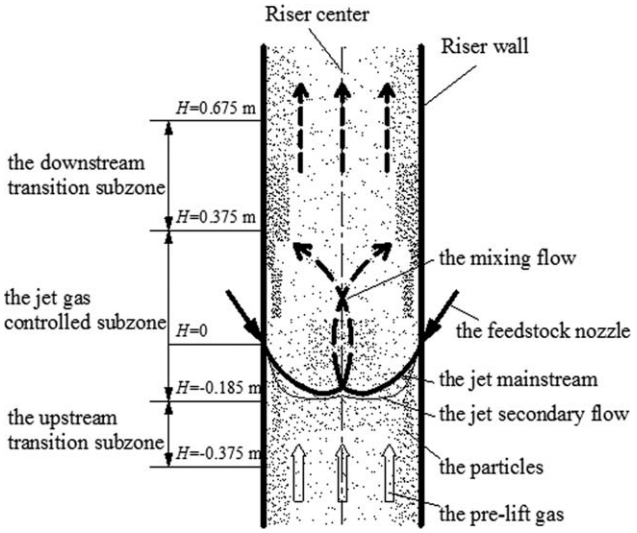

Figure 21. Mixing pattern in the new type of feed injection scheme.

between 40 and 80 m/s. In Figure 20, the nozzle spray velocity is fixed at 60 m/s and the prelift gas velocity is varied between 2 and 4 m/s.

When the nozzles are installed upward, the main stream reaches the riser center easier for high velocity of the feed spray or a low velocity of the prelift gas. However, the influence region of secondary flow expands more at these conditions. The velocity of feed jets and prelift gas should neither be too large nor too small. We are proposing $U_a \approx 3$–3.5 m/s and $U_j \approx 60$–70 m/s.

When the nozzles are installed downward, the ability of the main flow and secondary flow to reach the riser center is lessened when the velocity of feed jets is too large or the velocity of prelift gas is too small. Thus, the velocity of the feed spray should not be too large and the velocity of prelift flow should be properly increased within the operating conditions. We are proposing $U_a \approx 3.5$–4 m/s and $U_j \approx 50$–60 m/s.

Analysis of the mixing process

Based on the above discussion, the mixing process of the feed spray and the prelift gas-solid flow in the new type of feed injection scheme (feed nozzles are installed downward) illustrated in Figure 21 is proposed. Note that the calculation method of spray trajectories is only suitable for the region when the multiple feed jets do not meet. The centerlines of the jet main flow and the secondary flow are shown by solid lines while the trajectory of the mixed flow is denoted by the dashed lines after the multiple jets mix together.

In the traditional feed injection scheme, a secondary flow also forms near the riser wall accompanying the jet main stream when the feed spray is injected into a riser. The difference is that when the nozzles are installed downward the direction of secondary flow is toward the riser center while in the traditional scheme the direction is toward the riser wall. So in the new downward injection scheme, the feed spray covers the whole cross section of riser sooner. Furthermore, catalyst particles are transported to the riser center from the riser wall by the effect of main stream and secondary flow. Therefore, mixing and reaction of oil with catalysts in the initial contact region are significantly improved.

The main flow and secondary flow from the multiple feed jets mix with the prelift flow in the riser core area. The mixed flow promotes transport of catalyst particles toward the wall. As a result, dense regions form near the riser wall above the nozzles, which can adversely affect the reaction of oil with the catalyst. This disadvantage needs to be resolved.

Following the analysis of the trajectories of main jet flow and secondary flow in the initial contact region of oil with catalysts and with knowledge of the characteristics of gas–solid two-phase flow in the feed injection zone, the new type of feed injection scheme can be divided into three subzones. These are the upstream transition subzone ($H = -0.375$ to -0.185 m), the jet gas controlled subzone ($H = -0.185$–0.375 m) and the downstream transition subzone ($H = 0.375$–0.675 m).

Conclusions

A new type of FCC feed injection scheme in which the feed oil contacts with catalyst particles countercurrently in a circulating fluidized bed riser is proposed. The dispersion of feed spray as well as the flow behaviors of particles in this new feed injection zone was experimentally investigated in a large scale cold-riser model and results were compared with those of traditional co-current feed injection schemes.

The feed spray is simulated in the tests using Helium gas (no oil was used). The helium tracer was detected and measured as it mixed with riser fluidizing gas. When the feed nozzles are installed downward (angle $> 90°$ from vertical), the feed spray is in countercurrent contact and mixing with the prelift flow. As a result, the concentration distributions of feed jets and catalyst particles in the initial contact region of oil with catalysts are more uniform than that in the traditional scheme. The local and average catalyst-oil matching index is proposed to compare the match between oil and catalysts in the new and traditional feed injection zone. The results show that the cross sectional area average catalyst-oil matching index is smaller in longer sections of the feed zone when the feed are injected downward, which indicates that the new type of feed injection scheme provides a better contact between the feed oil and catalyst particles. The influence height of the feed spray above the nozzles decreases considerably.

The trajectories of the feed main flow and secondary flow were calculated. The density correction coefficient is used to correct the ideal condition. The results show that the trajectory of the feed secondary flow is toward the riser wall when the feed nozzles are installed upward while its direction is toward the riser center when the feed is injected downward. Similar results have been reported by studies that used the Kutta–Joukowski theorem. The influences of spray injection angle, spray velocity, and the riser prelift gas velocity on the spray trajectory were also determined.

Limitations and Future work

In this cold model experimental research, the operating parameters should be in accordance with those of the industrial riser reactor simultaneously. These parameters are the momentum ratio of the feed jet to the prelift flow, the volume flow ratio of the feed jet to the prelift flow, the velocity ratio of the feed jet to the prelift flow, the velocity at the nozzle exit, and the total superficial gas velocity in the feed injection zone. However, it is very hard to keep these five parameters in accordance with those of the industry case at the same time because of the very complex process in the actual feed injection zone as well as some differences between experiment and

industry. In this research, we tried our best to make the following conditions the same as the industry: the velocity at the nozzle exit, the velocity ratio of the feed jet to the prelift flow and the total superficial gas velocity in the riser after the feed jets mix with the prelift flow.[8,28] Thus, the feed jet is used the atmospheric air here and we think it is relatively reasonable as described in the Experimental setup section.

Limited to the difference between the atmospheric air and the real oil, the momentum ratio of jet injection to that of prelift gas in this article cannot keep the same as that of the industry. In the typical industry case, the momentum of the feed injection will change with time and the density of the feed cannot keep constant. Thus, it is very hard to give the accurate result of the industry case. Frankly, the large cold model experimental results perhaps cannot directly proposed the very precise information because some differences between experiment and industry are inevitable. However, the contacting/mixing process of feed with catalyst particles in both systems can be revealed via cold model experiment. The results of this research have given the gas-solid flow behaviors in the proposed feed injection scheme and its advantages have been shown. We plan to combine the cold model experiments with the numerical simulation as well as the industrial operation/experiments in our future research to make a better understanding of the scale-up of the industrial processes.

The residence time of feed jets is also an important parameter in the feed injection zone of FCC riser reactor. However, the residence times we obtained in this experiment are quite different from the residence time in the traditional chemical engineering as discussed in the Measurements and data analysis section. In the future work, we are going to establish the connection among these residence times.

Acknowledgment

The authors gratefully acknowledge the supports from the National Key Basic Research Development Project (973 Program) of China: No. 2012CB215000.

Notation

A = area, m^2
b = half width of jet, m
c = tracer concentration at i position
C_0 = eigen-concentration of feed spray
C_n = aerodynamic drag coefficient
D_r = diameter of riser, m
$F^{(e)}$ = principal vector of external force, N·m
H = axial height, m
K_D = density correction coefficient
M = momentum, kg m/s
m = mass, kg
N = number of measured points
n = the momentum ratio of the secondary flow to the main flow
p = pressure, Pa
Q = volumetric flow rate, m^3/s
R = radius of riser, m
r = distance to the riser center
U = velocity of jet at any location, m/s
u = velocity of gas, m/s
u_r = relative velocity, m/s
v = component velocity of Y axial, m/s
v_e = entrainment velocity of jet, m/s
x = horizontal coordinate of jet centerline in ideal condition, m
$\hat{x}$ = main stream centerline, m
$\hat{x}'$ = secondary flow centerline, m
y = longitudinal coordinate of jet centerline in ideal condition, m
$\hat{y}$ = of main stream centerline, m
$\hat{y}'$ = of secondary flow centerline, m

Greek letters

α = the angle of nozzle axis relative to the upward of riser axial
β = the angle of secondary flow relative to the upward of riser axial
Δ = change value
ε = volume fraction
ε_0 = eigen-volume fraction
θ = angle between tangential direction of element and centerline of jet
λ = local Catalyst-oil matching index
λ_m = average Catalyst-oil matching index
$\bar{\lambda}$ = atalyst-oil matching index
ρ = density, kg/m^3
τ = shear stress, N/m^2

Subscript

a = the prelift flow
c = the cavity caused by the jet
e = experimental data
i = position i
j = nozzle spray
p = particle

Literature Cited

1. Zhu C, Jun Y, Patel R, Wang D. Interactions of flow and reaction in fluid catalytic cracking risers. *AIChE J*. 2011;57:3122–3131.
2. Chen YM. Recent advances in FCC technology. *Powder Technol*. 2006;163:2–8.
3. He P, Zhu C, Ho TC. A two-zone model for fluid catalytic cracking riser with multiple feed injectors. *AIChE J*. 2014;61:610–619.
4. Helmsing MP, Makkee M, Moulijn JA. Short contact time experiments in a novel benchscale FCC riser reactor. *Chem Eng Sci*.1996; 51:3039–3044.
5. Al-Sherehy F, Grace J, Adris AE. Gas mixing and modeling of secondary gas distribution in a bench-scale fluidized bed. *AIChE J*. 2004;50:922–936.
6. Marzocchella A, Arena U. Hydrodynamics of a circulating fluidized bed operated with different secondary air injection devices. *Powder Technol*. 1996;87:185–191.
7. E C, Fan Y, Zhang K, Zhang H. Concentration profile of jet gas in the feed injection zone of a FCC riser. *Prog Nat Sci*. 2008;18:1285–1291.
8. Fan Y, Ye S, Chao Z, Lu C, Sun G, Shi M. Gas–solid two-phase flow in FCC riser. *AIChE J*. 2002;48:1869–1887.
9. Thelogs KN, Markatos NC. Advanced modeling of fluid catalytic cracking riser-type reactors. *AIChE J*. 1993;39:1007–1014.
10. Thelogs KN, Nikou I, Lygeros AI, Markatos NC. Simulation and design of fluid catalytic cracking riser-type reactors. *AIChE J*. 1997; 43:486–498.
11. Thelogs KN, Nikou I, Lygeros AI, Markatos NC. Simulation and design of fluid-catalytic cracking riser-type reactors. *Comput Chem Eng*. 1996;20:S757–S762.
12. Gao J. *Numerical Simulation on the Flow, Heat-Transfer and Reaction in the Catalytic Cracking Riser Reactors*. Ph.D. Thesis. Beijing: China University of Petroluem, 1997.
13. Gao J, Xu C, Lin S, Yang G, Guo Y. Simulations of gas-liquid-solid 3-phase flow and reaction in FCC riser reactors. *AIChE J*. 2001;47: 677–692.
14. Li J, Fan Y, Lu C, Luo Z. Numerical simulation of influence of feed injection on hydrodynamic behavior and catalytic cracking reactions in a FCC riser under reactive conditions. *Ind Eng Chem Res*. 2013; 52:11084–11098.
15. Li J, Luo Z, Lan X, Xu C, Gao J. Numerical simulation of the turbulent gas-solid flow and reaction in a polydisperse FCC riser reactor. *Powder Technol*. 2013;237:569–580.
16. Patel R, Wang D, Zhu C, Ho TC. Effect of injection zone cracking on fluid catalytic cracking. *AIChE J*. 2013;59:1226–1235.
17. Pan L, Yuan H, Nie B. Optimized technology for residuum processing in the ARGG unit. *China Pet Process Petrochem Technol*. 2006; 2:25–31. (in Chinese)
18. Long J, Tian H, Liu Y, Xie C, Li J. Study on the performance and application of new generation DMMC-1 type catalyst for deep catalytic cracking. *China Pet Process Petrochem Technol*. 2007;4: 1–6.

19. Zhang J. Development and application of DCC catalysts to meet new demands. *China Pet Process Petrochem Technol*. 2013;1:14–18. (in Chinese)
20. Xu Y, Zhang J, Long J, He M, Xu H. A modified FCC process for maximizing isoparaffins (MIP) in cracked naphtha. *Acta Petrolei Sin*. 2003;19:43–47. (in Chinese)
21. Li C, Yang C, Shan H. Maximizing propylene yield by two-stage riser catalytic cracking of heavy oil. *Ind Eng Chem Res*. 2007;46: 4914–4920.
22. Gan J, Zhao H, Berrouk A, Yang C, Shan H. Numerical simulation of hydrodynamics and cracking reactions in the feed mixing zone of a multiregime gas-solid riser reactor. *Ind Eng Chem Res*. 2011;50: 11511–11520.
23. Maroy JD. Process and apparatus foe contacting a hydrocarbon feedstock with the hot solid particles in tubular reactor with a rising fluidized bed. *U.S. Patent 5348644*, 1994.
24. Zheng M, Hou S, Zhong X, Li S. Determining the particle velocity distribution in FCC riser with different structures. *Pet Process Petrochem (in China)*. 2000;31:45–51. (in Chinese)
25. Dries HWA. Reactor riser for fluidized-bed catalytic cracking plant. *U.S. Patent 6596,42*, 2003.
26. Lomas DA, Haun EC. FCC riser with transverse feed injection. *U.S. Patent 5139748*, 1992.
27. Li T, Guenther C. A CFD study of gas-solid jet in a CFB riser flow. *AIChE J*. 2012;58:756–769.
28. Fan Y, E C, Shi M, Xu C, Gao J, Lu C. Diffusion of feed spray in fluid catalytic cracker riser. *AIChE J*. 2010;56:858–868.
29. Mauleon JL, Sigaud JB. Process for the catalytic cracking of hydrocarbons in a fluidized bed and their applications. U.S. Patent 4883583, 1989.
30. Chen S, Wang W, Yan Z, Fan Y, Lu C. Numerical simulation on flow and mixing of gas-solid two-phase in FCC riser feedstock injection zone by using EMMS drag model. *2014 Technical Congress on Resources, Environment and Engineering*. Hong Kong, 2014.
31. Dong Q, Feng M, Qiu DK, Yu T. Research progress of FCC feeding nozzle technique. *J Chem Ind Eng*. 2012;33:31–37. (in Chinese)
32. Diu D, Han J. Evaluation on commercial application of LPC type nozzle for FCC feed. *Pet Refinery Eng*. 1992;2:49–52. (in Chinese)
33. Yan C, Lu C, Liu Y, Cao R, Shi M. Hydrodynamics in airlift loop section of petroleum coke combustor. *Powder Technol*. 2009;192: 143–151.
34. Zhu L, Fan Y, Lu C. Mixing of cold and hot particles in a prelifting scheme with two strands of catalyst inlets for FCC riser. *Powder Technol*. 2014;268:126–138.
35. Cao C, Weinstein H. Gas dispersion in downflowing high velocity fluidized beds. *AIChE J*. 2000;46:523–528.
36. Du B, Fan LS, Wei F, Warsito W. Gas and solids mixing in a turbulent fluidized bed. *AIChE J*. 2002;48:1896–1909.
37. Nieuwland JJ, Meijer R, Kuipers JAM, van Swaaij WPM. Measurements of solids concentration and axial solids velocity in gas-solid two-phase flows. *Powder Technol*. 1996;87:127–139.
38. Chen G, Luo Z. New insights into intraparticle transfer, particle kinetics, and gas-solid two-phase flow in polydisperse fluid catalytic cracking riser reactors under reaction conditions using multi-scale modeling. *Chem Eng Sci*. 2014;109:38–52.
39. Sawyer RA. The flow due to a two-dimensional jet issuing to a flat plate. *J Fluid Mech*. 1960;9:543–560.
40. Eriksson JG, Karlsson RI, Persson J. An experimental study of a two-dimensional plane turbulent wall jet. *Exp Fluids*. 1998;25:50–60.
41. Shantanu P, Manab Kumar D. Computational study of a turbulent wall jet flow on an oblique surface. *Int J Numer Method Heat Fluid Flow*. 2014;24:290–324.

Manuscript received May 22, 2015, and revision received Aug. 7, 2015.